ACS Sustainable Chemistry & Engineering

pubs.acs.org/journal/ascecg

Research Article

The Future is Garbage: Repurposing of Food Waste to an Integrated Biorefinery

Elvis Ebikade, Abhay Athaley, Benjamin Fisher, Kai Yang, Changqing Wu, Marianthi G. Ierapetritou, and Dionisios G. Vlachos*

Cite This: https://dx.doi.org/10.1021/acssuschemeng.9b07479

Read Online

ACCESS | Metrics & More | Article Recommendations | Supporting Information

ABSTRACT: Globally, 1.3 billion tons of food is wasted annually, with few uses other than landfilling, anaerobic digestion, or composting. Food waste (FW) repurposing provides an alternative waste management strategy toward meeting goal 12 of the United Nations sustainable development goals. Here, we present an integrated biorefinery technology, repurposing potato peel waste (PPW) for manufacturing multiple biobased value-added products. We report an integrated biorefinery comprising three stepwise processes: ultrasonic extraction to recover extractives for high activity antioxidants' production, optimized hydrolysis and dehydration of glucose resulting in the highest reported yields (54%) of 5-hydroxymethylfurfural (HMF), directly from potato peels, for manufacturing biobased chemical precursors, and finally, pyrolysis of the residual lignin into biochar for remediating pesticide contaminated water, improving water quality. As a best-case scenario, we obtain revenues of about $6300 per MT of dry PPW. This provides the opportunity for successful translation of our technology to an economically profitable process using zero value food waste. This study provides a sustainable valorization blueprint that can be extended to other types of FW for improving the economics of biomass-based biorefineries by manufacturing multiple renewable products.

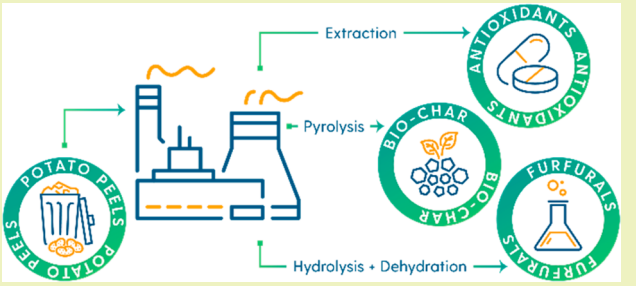

KEYWORDS: *Food waste, Biorefinery, Circular economy, Antioxidants, Hydroxymethylfurfural, Biochar, Techno-economics, Sustainability*

INTRODUCTION

Global food waste (FW) is currently estimated to be 1.3 billion tons annually,[1] roughly one-third of global food production. This number is expected to surge higher with further economic and global population increase. The National Academy of Sciences, Engineering and Medicine's report[2] identifies FW as one of the key challenges facing the US food and agriculture (Figure 1) and states, "Further innovation to reduce and repurpose FW is needed because the United States wastes approximately $278 billion annually, which is enough to feed nearly 260 million people".[2] The magnitude of FW as well as its sustainability, energy content loss, and financial impacts are described in Figure 1. On a global scale, ~$1 trillion[1] worth of food with an energy content (average food waste calorie content of 4 kcal/g) of 26 ExaJoules (a quarter of US energy consumption[3]) is wasted annually. If FW was a country, it will be the third largest greenhouse gas emitter behind China and the US.[4]

With 83% of FW (Figure 2a) ending up in landfills,[5] repurposing FW as a feedstock for valuable products combats part of the challenge associated with the current FW management strategies. Toward this goal, the United States Department of Agriculture (USDA), the Environmental

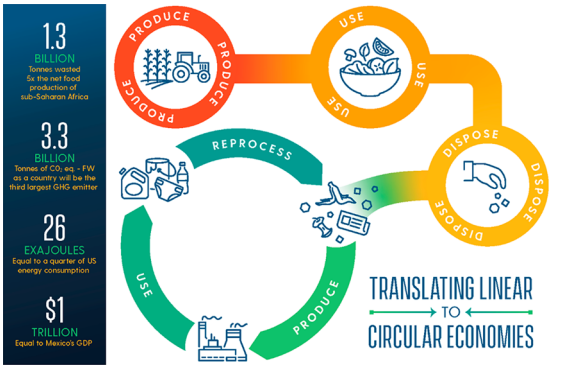

Figure 1. Food waste scale and innovation challenge. Scope and potential of transforming existing FW management linear economy into a circular economy for producing societal goods.

Received: December 14, 2019
Revised: March 24, 2020
Published: May 12, 2020

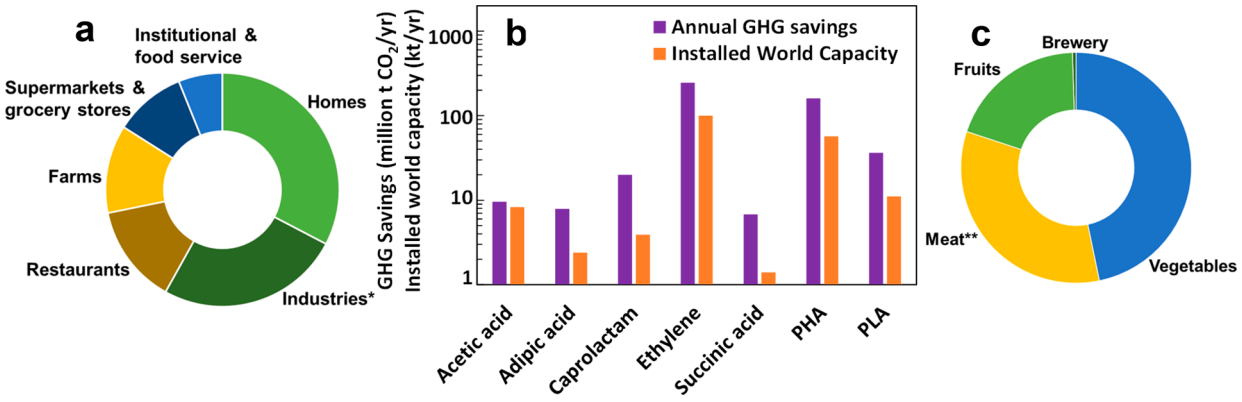

Figure 2. Scale of opportunity. (a) Breakdown of FW generation (83 million tons) by supply chain stage in the US.[7] (b) Greenhouse gas (GHG) savings potential[18] when replacing petrochemicals (global production volume on secondary *y*-axis) with bioalternatives. On the basis of world production capacity in years 1999/2000, not accounting for chemical industrial growth, and without including reduction in biodiversity impact, groundwater pollution, and soil fertility effects. PHA: Polyhydroxyalkanoates. (c) Breakdown of US industrial FW into key sectors,[8] without including waste used for animal feed. Main vegetable waste: potato, tomato, and corn; main fruit waste: banana, apple, and grape. *95% used for animal feed, composting, anaerobic digestion or energy generation. **Solid waste from meat processing consists primarily of slaughterhouse waste.

Protection Agency (EPA), and the Food and Drug administration (FDA) recently signed a federal interagency strategy to reduce and redirect food waste away from landfills.[6] Prior efforts to manage FW include use for animal feed,[5,7] composting,[8,9] anaerobic digestion,[10,11] and fermentation,[12,13] but their economic viability can be a challenge. In contrast, the conversion of agricultural and food-processing waste to bulk chemicals can be nearly 10, 7.5, and 3.5 times more profitable than its use for electricity generation, animal feed, and transportation fuel, respectively.[14,15] This economic fact, combined with the proposal of USDA and the Department of Energy (DOE) to increase biobased commodity chemicals and materials from 5% in 2005 to 25% in 2030,[16] define a new paradigm of FW-repurposing, moving from a lignocellulose-centric biorefinery approach to one that incorporates FW for manufacturing biobased products. Given the substantial investment of the US in creating biorefineries utilizing lignocellulosic plant material for second generation fuels and bioproducts, a large fraction of FW could be diverted into biorefineries if suitable technologies were available.[17] A collateral benefit is the potential greenhouse gas savings[15] incurred by switching from petrochemicals to biochemical alternatives made from biomass (lignocellulose and FW) in a biorefinery[15] (Figure 2b).

According to the FAO,[19] global potato production is estimated to be 388 million tonnes. Asia and Europe account for 80% of this global production with China being the largest potato producer. Following current production trends, these numbers are increasing (Figure S1). In the US, potatoes are the most consumed vegetable[20] (Figure 2c). Approximately 2−6 million tons of PPW are produced annually, accounting for 3% of the total US FW stream.[16] US landfills accounts for 18% of the total U.S. methane emissions.[21] When PPW is not used as animal feed, it ends up at landfills, where it takes up space and contributes to these emissions. Liang et al. have studied the bioconversion of PPW into lactic acid[22] and Arapoglou et al. investigated PPW fermentation into ethanol[13] as potential PPW biorefinery products. PPW can provide three times the required amount of glucose needed to meet the global demand for lactic acid, succinic acid, fumaric acid, and polyhydroxybutyrate.[9,23] The continuous supply, relatively homogeneous composition and isolated stream of industrial PPW make it an excellent biorefinery feedstock, circumventing sorting and landfill gate fees.

Here, we develop a multiple-conversion FW strategy: PPW extraction to recover extractives for antioxidants' production, hydrolysis combined with simultaneous glucose dehydration into 5-hydroxylmethyl furfural (HMF), one of the key platform chemicals defined by DOE,[24] and pyrolysis of the residual lignin into biochar for treating pesticide contaminated water. This introduces a new strategy for repurposing FW in an integrated biorefinery where FW and lignocellulose can be (co)processed to produce a slate of products analogous to a conventional refinery. Techno-economic analysis (TEA) highlights the economic viability of repurposing PPW as a nonconventional feedstock for manufacturing value-added products. This approach ensures exhaustive and cost-effective valorization of PPW, introducing a symbiosis between FW and chemical industry, and importantly, provides a conceptual framework for feedstock diversification of biorefineries and bioenergy more generally, whereby FW and lignocellulose-plant material can be used separately or integrated.

EXPERIMENTAL SECTION

Materials. Potato starch from Sigma-Aldrich was used as a substrate in creating the standard glucose solutions for the design of experiments. Butanol, ethyl acetate, methyl isobutyl ketone (MIBK), $AlCl_3$, LiBr, and H_2SO_4 were purchased from Sigma-Aldrich. Methanol (HPLC grade) and dimethyl sulfoxide (DMSO) were purchased from Fisher Chemical, Fisher Scientific, United States. Absolute ethanol (molecular biology grade) was purchased from Fisher Bio reagents. Folin-ciocalteau's phenol reagent, 6-hydroxy-2, 5, 7, 8-tertramethlchroman-2-carboxylic acid (Trolox), 2, 2-diphenyl-1-picrylhydrazyl (DPPH), chlorogenic acid, and *p*-Coumaric acid (≥98%, HPLC grade) were purchased from Sigma-aldrich. Inc. (St. Louis, MO). Gallic acid and 2, 2-azobis (2-methylpropionamidine) dihydrochloride (AAPH) were purchased from Acros (New Jersey, USA). Gallic acid (98%, Acros-Organics), caffeic acid (≥95%, HPLC grade, Fluka), quercetin dihydrate (95%, MP Biomedicals, LLC), formic acid (LC-MS grade, Fisher Chemical). 1,2 Dibromo-chloro-propane (DBCP) was obtained as a 5000 mg/L solution in methanol (Sigma-Aldrich). All chemicals were used as received. Deionized water (Millipore model Direct Q3 UV R) was used for the preparation of all solutions. Syringe filter discs (Nylon, 0.2 μm) for the filtration of samples prior to HPLC analysis were purchased from Fisher Scientific.

https://dx.doi.org/10.1021/acssuschemeng.9b07479
ACS Sustainable Chem. Eng. XXXX, XXX, XXX−XXX

Sample Preparation. The potato (Russet Burbank) sample was purchased from ACME store, rinsed with water, and peeled using a manual peeler. We used a Russet Burbank potato variety (same used by large brands like Lays and Herr's for making potato chips) to ensure semblance to industrial PPW. The peeling procedure we applied mimics the abrasion process used in potato chips processing. The peels were dried in a vacuum oven below 50 °C until the moisture content was below 10 wt % according to NREL LAP NREL/TP-510-42620. The dried peels were then ground in a ceramic mortar and sieved to collect <0.5 mm particle size powdered peels. The powdered peels were kept in an airtight storage container at room temperature. Moisture content of the powdered peels was determined by a Sartorius moisture content analyzer. All physicochemical characterization data were calculated on a dry weight basis.

Fractionation of Extractives from PPW. The ultrasound assisted procedure was used for the extraction of potato peel in a 50:50 methanol and water mixture. Thus, 20 mL of solvent was added to 1 g powdered peels, the mixture was sonicated in an ultrasonic bath for 15 min. The extract was filtered using a gooch funnel for removal of peel particles and the supernatant was centrifuged at 3000 × *g* for 10 min at 5 °C and stored in a refrigerator.

Test of Total Phenolics Content (TPC). The concentration of total phenolic compounds was determined using the methods described by Wu et al.[25] The gallic acid standards were dissolved in absolute ethanol diluted to the different concentration using DI water. Then 20 μL of the extracts or standards were mixed with 180 μL of distilled water, 100 μL of Folin-ciocalteau reagent, and 0.5 mL 20% sodium carbonate solution. The samples were allowed to stand at room temperature for 2 h. The absorbance was read at 765 nm by the Synergy 2 multimode microplate reader (BioTek Instruments, Inc., Winooski, VT). A calibration curve using gallic acid was used to derive the gallic acid equivalent (GAE) concentrations for samples. The results were expressed as milligrams (mg) of gallic acid equivalents (GAE) per g of dried PP extractives (PPE) or mg GAE per g of dried potato peel (PPW).

Measurement of DPPH Free-radical Scavenging Effect. DPPH scavenging effects were determined by modified methods as reported by Wu et al.[26] A 500 μL aliquot of a solution of 500 μM DPPH radicals was mixed with 500 μL of each diluted extract or standard solution. A control reaction mixture was prepared without any extract, sample blanks were included with addition of the same volume of DMSO instead of DPPH solution, and Trolox was used as the reference standard. The mixture was shaken vigorously and left in the dark at room temperature for 20 min. The changes of absorbance were measured at 517 nm using the Synergy 2 multimode microplate reader (BioTek Instruments, Inc., Winooski, VT). The results were expressed as the mmol Trolox equivalents (TE) per g of PPE or mmol TE per g of PPW.

Hydrophilic Oxygen Radical Absorbance Capacity (ORAC) Assay. The ORAC assay was performed using the same Synergy 2 multimode microplate reader equipped with an incubator and two injector pumps, with the method previously reported by Dong et al.,[27] with slight modification. An aliquot of 25 μL of samples or Trolox standard solution were added into wells of 96-well black microplate with clear bottom. To each well, 150 μL of fluorescein (0.004 μM) in 75 mM phosphate buffer (pH 7.4) was added), and the mixture was incubated for 1 h at 37 °C inside the reader, before injection of 25 μL of 153 mM AAPH solutions to start the reaction. The microplate reader was then programmed to record the fluorescence reading with an excitation wavelength of 485 nm and an emission wavelength of 520 nm at 1 min intervals for 1 h. The standard curve was linear between 0 (phosphate buffer, pH 7.4) and 100 μM Trolox. Results were expressed as mmol TE per g of PPE or mmol TE per g of PPW.

HPLC Analysis of Potato Peel Extractives (PPE). Analysis was performed on a Shimadzu Prominence HPLC system, equipped with LC-20AT quaternary gradient pump, SPD-M20A diode array detector (DAD), CBM-20A communication bus module, CTO-10AS VP column oven, SIL-20AT autosampler, and Shimadzu Ezstart 7.4 software. Separation was carried out on an XBridge C18 column (150 mm × 4.6 mm, 3.5 μm, Waters, Ireland), at column temperature of 35 °C and a flow rate of 1.0 mL/min using solvent A (aqueous 1% formic acid) and solvent B (100% methanol) with a linear gradient elution: starting with 5% B in order to reach 40% B at 10 min, 60% B at 15 min, 80% B at 20 min, and 100% B at 25 min. Phenolics were detected at 280 and 325 nm. Compounds were identified and quantified by conventional retention time and integration area using standards. Standards include chlorogenic acid, caffeic acid, gallic acid, ferulic acid, *p*-coumaric acid, and quercetin dehydrate.

Selection of Organic Solvents for Reactive Extraction. 2-Butanol, ethyl acetate, and MIBK were selected as green organic solvents for HMF based on the green chemistry solvent selection guide.[28,29] The subsequent screening criteria were based on reactivity of organic phase with HMF (measured by HMF mass conservation on heating in organic phase) and partition coefficient of HMF in organic solvents. These experiments were performed in high pressure glass reactor placed in a preheated stainless-steel heating block. To measure the reactivity of the organic phase (Figure S12) with HMF, 1 wt % HMF in each organic solvent was heated at 140 °C for 1 h. The concentration of HMF was measured before and after the reaction. For the partition experiments, to a mixture of 1 mL of 1 wt % HMF in 25 wt % LiBr + 0.05 M H_2SO_4 was added 1 mL of organic solvent. This mixture was heated at 140 °C for 1 h. The concentration of HMF in both phases after the experiment was quantified and used to determine the extraction ratio. While ethyl acetate and 2-butanol showed the least amount of side reactions with HMF, ethyl acetate formed a single phase with the aqueous phase after reaction at 140 °C. After selection of 2-butanol as the organic solvent, a calculated amount of 2-butanol was added to adjust the ratios of organic and aqueous phase between 1 and 4 (v/v) to evaluate the effect of the volume of the extracting solvent on HMF partitioning (Figure S13). The mixture was stirred at 140 °C for 1h and settled overnight to ensure complete phase separation. HMF concentrations in both phases were quantified by HPLC upon dilution. All experiments were conducted in duplicate.

Saccharification of Extracted PPW. Saccharification of extracted PPW was conducted in high-pressure glass vials. Each vial was loaded with a calculated amount of LiBr and 0.05 M H_2SO_4. Upon dissolving LiBr, the calculated amount of extracted PPW was added into the vial and the mixture was vortexed for about 30 s. A magnetic bar was added for stirring. The vial was sealed with a needle valve adaptor and placed in a preheated heating block to start saccharification at 140 °C. Upon completion of the reaction for the set time, the vial was removed from the heating block and quenched in an ice bath. A portion of the hydrolysate was diluted in DI water 10 times and filtered for HPLC analysis.

Preparation of Standard Glucose Hydrolysate. A 0.06 g portion of potato starch was added into high pressure glass tubes and filled with 2 mL of a 25 wt % LiBr and 0.05 M H_2SO_4 solution. The tubes were then sealed and placed in a preheated heating block stirred for 1 h at 140 °C to convert the starch into glucose. This standard glucose solution was then run on the HPLC to determine its glucose concentration. This stock solution was used for the glucose dehydration experiments specified by the experimental design.

Dehydration. Glucose in the hydrolysate, obtained from starch or extracted PPW was dehydrated to HMF in a biphasic system. Typically, hydrolysate (0.5 mL) was mixed with a calculated amount of a Lewis acid ($AlCl_3$) and an organic-extracting solvent (2-butanol) in a high-pressure glass tube. The ratio of the hydrolysate (reactive phase) to organic solvent was of 1:3 (v/v). Upon addition of a small magnetic bar into each tube for stirring, the tubes were sealed and placed in a preheated heating block preset at the desired temperature. After completion of the reaction for the set time, each tube was removed from the heating block and quenched in an ice bath. The solution was allowed to settle to ensure separation of the two phases. Both aqueous and organic phases were filtered for analysis by HPLC. The aqueous phase was diluted 10 times with DI water before HPLC analysis.

Factorial Experimental Design and Optimization of Parameters for Glucose Dehydration. Temperature, Lewis acid catalyst ($AlCl_3$) concentration, and reaction time were chosen as independent

https://dx.doi.org/10.1021/acssuschemeng.9b07479
ACS Sustainable Chem. Eng. XXXX, XXX, XXX−XXX

variables. Each variable had three different levels consisting of low, medium, and high. The statistical analysis of HMF yield (response variable) was analyzed using the Minitab 18 software. The experimental range and levels of independent variables for HMF production are given in Table S1. A Box-Behnken design was used to predict the conditions that would give the maximum HMF yield and to study the interaction of the significant factors. This design was implemented due to its exclusion of extreme values of factors, which makes running the design of experiments easier and more cost-effective. The design of experiments was run with two replicate experiments resulting in 30 total experiments. The regression equation predicting HMF yield was determined using Minitab. The complete design matrix of the Box-Behnken design is shown in Table S2.

Recycling of Aqueous Phase. Recyclability of the 25 wt % LiBr + 0.05 M H_2SO_4 was tested for potato starch hydrolysis to yield soluble glucose sugar. After starch hydrolysis at 140 °C for 1 h, the hydrolysate containing soluble glucose was subjected to dehydration in 25 wt % LiBr + 0.05 M H_2SO_4-2-butanol (1:3 volume ratio) biphasic system at 160 °C for 3 h using $AlCl_3$ (0.8 mol ratio to glucose in solution). After separation of the organic phase containing HMF and washing the aqueous phase twice with 2-butanol, the recovered aqueous phase, containing 25 wt % LiBr + 0.05 M H_2SO_4 and Al species, was filtered through a syringe filter and reused in a second cycle. The yields of glucose and HMF after the hydrolysis and the dehydration steps were quantified by HPLC. For the second cycle, the unconverted glucose in the hydrolysate after the first cycle of dehydration was accounted for when adding starch for hydrolysis in the second cycle. 2-Butanol was added to adjust the ratio of 2-butanol to aqueous phase to 3:1 volume ratio and the mixture was heated at 160 °C for 2 h. Starch hydrolysis and glucose dehydration took place simultaneously in the second cycle as the recovered aqueous phase from the first cycle contained both Brønsted (25 wt % LiBr + 0.05 M H_2SO_4) and Lewis acid ($AlCl_3$) catalysts. Upon completion of the second cycle, the organic and aqueous phases were processed as described above and the reactive phase was reused.

Analysis and Quantification of Hydrolysis and Dehydration Products. Sugar hydrolysates and the aqueous and organic phases from sugar hydrolysates dehydration reactions were diluted 10 times, unless otherwise mentioned, and analyzed on a Waters HPLC instrument (model e2695) equipped with a photodiode array (PDA) detector (Waters 2998) as well as a refractive index (RI) detector (Waters 2414). Two HPLC columns of the following specifications were used for analysis of different sugar and furfurals products at different operating conditions: (1) A Biorad Aminex HPX-87H (7.8 × 300 mm, 9 mm) column operating at column oven temperature of 55 °C, an aqueous solution of H_2SO_4 (0.005M) as a mobile phase at flow rate of 0.6 mLmin^{-1} was used for detection and quantification of glucose (9.52 min), fructose (10.26 min), and HMF (30.22 min), using a PDA detector (254 nm). The number in parentheses refers to the retention time of the species. An Agilent Zorbax SB C18 (4.6 × 250 mm, 5 mm) column operating at column oven temperature of 25 °C and acetonitrile/water mixture (1:1 v/v) as a mobile phase at a flow rate of 0.2 mL min^{-1} was used for analysis of HMF in the organic phase from sugar hydrolysates dehydration experiments using a PDA detector (320 nm). The characteristic peaks for organic products and sugar monosaccharides and oligosaccharides were identified from the retention times of the authentic samples. Each peak was integrated, and the actual concentrations of each product were calculated from their respective precalibrated plots of peak areas vs concentrations.

Pyrolysis of Recovered PPW Residue to Biochar. The PPW residue was exposed to a combined thermal stabilization/pyrolysis step followed by passivation. A tube furnace (Thermo Scientific Lindberg Blue M model) was setup with inert gas conditions contained the recovered PPW residue in a quartz boat crucible. During the thermal stabilization and pyrolysis step, the furnace was heated from 30 to 1000 °C in the presence of He at a rate of 10 °C min^{-1} and then held at 1000 °C for 1 h producing a biochar. The furnace was setup with a helium-hydrogen (He-H_2) gas mixture for the passivation step. Passivation was conducted by heating at 10 °C min^{-1} to a temperature of 1050 °C with a 1 h hold prior to cooling.

DBCP Adsorption Measurements. A 10 ml of 1, 5, 10, 25, 50, 100 mg/L solution of DBCP in deionized water was mixed with 10 mg of our synthesized biochar in 40 mL glass vials with Teflon-lined cap. Adsorption experiment was run in duplicate. The vials were placed on a shaker for 48 h. After contact, a portion of the solution was filtered and stored for DBCP quantification.

NMR Spectroscopy. ^{1}H NMR was recorded on an Avance III 400 MHz NMR spectrometer (Bruker). The solvent contained 500 μL of sample and 100 μL of D_2O (containing 4 ppm DMSO as internal standard), and data processing was performed using the Mestrelab Research software (mNOVA). The samples were prepared in quartz NMR tubes (NewEra) and were studied at 303 K.

Quantification of DBCP. NMR signals for H on carbon 1 (Figure S14) was used to quantify the concentrations of DBCP in solution. This corresponds to a chemical shift of 3.15 and 3.4 on the NMR spectra. An internal standard (4 ppm DMSO) was added to each sample before analysis. The signal for H on carbon 1 was integrated (chemical shift 3.15) and normalized by the peak area of the DMSO internal standard, accounting for variation in NMR spectra intensity between runs. The actual concentrations of DBCP in solution were estimated from their respective precalibrated plots of normalized signal areas vs. concentrations

Thermogravimetric Analysis. TGA was performed on samples (2 mg) using a TA Instruments Q600 SDT thermogravimetric analyzer and differential scanning calorimeter (DSC) using a temperature program of 20 to 1000 °C at a heating rate of 10 K min^{-1} under N_2 (30 mL min^{-1}).

BET Surface Area and Pore Size Measurement. BET measurement was performed using a micrometrics ASAP 2020 surface area and porosity analyzer. The biochar sample was freeze-dried in a Mill Rock technology freeze-dryer before BET analysis.

H_2O Adsorption Measurements. Water adsorption data were collected using a micrometrics ASAP 2020 surface area and porosity analyzer. The biochar sample was freeze-dried in a Mill Rock technology freeze-dryer before analysis.

X-ray Powder Diffraction (XRD) Characterization. The XRD patterns were collected at room temperature using a Bruker D8 Discover X-ray diffractometer using Cu Kα radiation (λ = 1.5418 Å) source. The data were collected in a stepwise fashion of 2θ ranging from 5° to 90° and a step size of 0.05° and 1 s per step.

Scanning Electron Microscopy (SEM). SEM analysis of PPW and lignin samples was performed on an Auriga 60 microscope (Carl Zeiss NTS GmbH, Germany) equipped with a Schottky Field Emission Gun (FEG). All samples were deposited on adhesive carbon tape and sputtered by a DESK IV sputter unit (Denton Vacuum Inc. NJ, USA) equipped with Au/Pd target.

Statistical Analysis. Statistical analyses of obtained data were conducted using the MINITAB software under analysis of variance (ANOVA) at an α level of 0.05 to determine significant differences between the measured properties.

Compositional and Structural Analyses of PPW. Ground PPW (10 g) were Soxhlet extracted with water and ethanol overnight according to NREL LAP NREL/TP-510-42619 and the amount of extractives were determined gravimetrically. The lignin fraction was divided into acid insoluble and acid soluble fractions. The acid insoluble and acid soluble fractions were analyzed according to NREL/TP-510−42618 and TAPPI method, respectively. Carbohydrate analysis was performed on the 2-stage acid-hydrolysis according to NREL LAP NREL/TP-510−42623. Starch content was determined using Megazyme total starch assay kit (AA/AMG) based on the AOAC Method 996.11. All sugars were analyzed by HPLC. The protein content was determined using the Dumas combustion method, using an Elementar Vario-Max CN analyzer (Elementar Americas, Mt Laurel, NJ). The ash content was determined by furnacing samples at 600 °C according to NREL LAP NREL/TP-510−42622. Elemental analysis of ash content was carried out using an EDX analyzer on a JEOL JSM 7400F scanning electron microscope.

https://dx.doi.org/10.1021/acssuschemeng.9b07479
ACS Sustainable Chem. Eng. XXXX, XXX, XXX−XXX

RESULTS AND DISCUSSION

Potato Peel Waste (PPW) Feedstock Characterization. PPW compositional analysis (see Methods) results are presented in Table 1. On dry weight basis, PPW contains ∼50 wt % carbohydrates (35 wt % starch and 19 wt % nonstarch polysaccharides), ∼ 20 wt % extractives, and ∼12 wt % lignin.

Table 1. Physico-Chemical Composition of PPW

Component	Amount (wt %)
Moisture	7.53 ± 0.85
Oven-Dried Sample (Zero Moisture)	
Ash	9.12 ± 0.13
Extractives	
Ethanol Extractives	4.94 ± 0.192
Water Extractives	17.94 ± 6.1
Carbohydrate	
Starch	35.40 ± 0.18
Glucan	15.83 ± 0.42
Xylan	1.04 ± 0.09
Galactan	2.48 ± 0.21
Acetate	0.52 ± 0.06
Lignin	
Acid Soluble Lignin	3.00 ± 0.07
Acid Insoluble Lignin	8.39 ± 0.44
Total (Oven dry weight)	**98.66 ± 5.2**

The peels contain a high ash content ∼9 wt %, typical of herbaceous plant material, consisting of inorganic elements, such as potassium, magnesium, calcium, and silicon (Figure 3a). With ∼90 wt % of PPW dry weight consisting of carbohydrates, extractives, and lignin, PPW provides an interesting feedstock for manufacturing value-added products.

Scanning electron microscopy (SEM) imaging shows the presence of oval shaped granular material (Figure 3b), typical of potato starch in dried PPW (Figure 3c). Selective enzymatic hydrolysis of starch removes the oval shaped granular material, leaving behind a fibrous-like material (Figure 3d), typical of lignocellulose. Imaging corroborates the physicochemical characterization, confirming the presence of starch and lignocellulose.

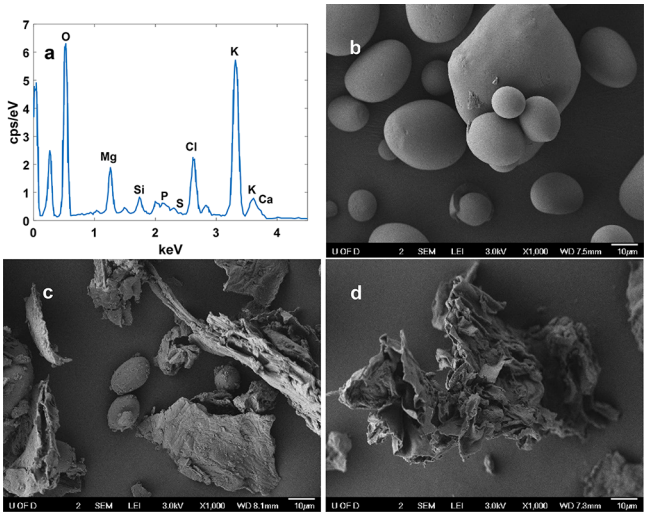

Figure 3. Physical characterization of PPW. (a) Energy-dispersive X-ray spectroscopy (EDX) analysis of PPW ash. (b) SEM of potato starch. (c) SEM of dried PPW showing lignocellulosic fibers and potato starch granules. (d) SEM of PPW after selective hydrolysis of starch.

Overall Multipronged Biorefinery Strategy. An attractive feature of our strategy (Figure 4) is the efficient repurposing of PPW components for producing bioproducts, providing an alternative to a make, use, and dispose linear economy and opening up a platform for circular economy by keeping resources in use for as long as possible, while extracting the maximum value from it (Figure 1). The multipronged approach entails first ultrasonic-assisted extraction of antioxidants, followed by one pot hydrolysis and dehydration of starch and cellulosic material, and finally by pyrolysis of lignin.

Our conversion process entails independent valorization of each component (extractives, carbohydrates, and lignin) to maximize their value toward manufacturing targeted products. Further processing of these components provides renewable alternatives to petroleum-derived products. After extracting PPW using water and methanol, the extracted peels are hydrolyzed in 25 wt % LiBr + 0.05 M H_2SO_4 to produce glucose, which is subsequently dehydrated to HMF in a biphasic reactive extraction system. Lithium bromide (LiBr) is used as an acid cocatalyst, increasing solution Brønsted activity with minimal corrosivity compared to a pure acid at equivalent pH.[30−32] The solid residue (after hydrolysis and dehydration of the carbohydrates in extracted PPW) is recovered and pyrolyzed to biochar.

Natural Antioxidants for Human Health. The antioxidant potential of PPW has been well studied.[33−38] Although these reports highlight its potential as a viable component for manufacturing antioxidants for dietary supplements, these have not been exploited in an integrated biorefinery. With extractives constituting ∼20% of PPW dry weight, manufacture of antioxidants from peels is economically attractive. Ultrasonic extraction is a simple, easy to handle and low cost alternative to Soxhlet extraction.[36−39] We performed ultrasonic extraction using an ethanol−water mixture, obtaining similar extractive yields (∼21 wt %) as with the methanol−water mixture. This indicates that any of the two solvents will effectively solubilize the extractives from PPW. Silva-Beltran et al.[37] showed that acidified ethanol extract had a total phenolic content (TPC) of 14.03 ± 1.88 mg gallic acid equivalent (GAE)/g potato peel extractives (PPE), and water extract had 1.02 ± 0.12 mg GAE/g PPE. The experimental findings on TPC (Table 2) were higher than prior reported values.[36−38] Albishi et al.[39] reported TPC in varieties of potato peel, ranging from 1.51 to 3.32 mg GAE/g PPW, which is less than the TPC of the water + methanol extract (6.90 ± 0.12 GAE/g PPW). The high phenolic content could be a result of ultrasonic−assisted extraction (improving solid−liquid contact) and low temperature drying of the peels (preventing degradation of some phenolic acids). As shown in Figure S5 and Table S1, four phenolic compounds, namely, chlorogenic acid, caffeic acid, *p*-coumaric acid, and ferulic acid, were quantified in the extracts, with the former two being dominant, corroborating prior results.[37,39] Gallic acid and quercetin were not found in the samples.

Three unknown peaks in retention time of 12−14 min were fully separated by slightly modifying the gradient elution procedure of Albishi et al.[39] The ratio of free chlorogenic acid to free caffeic acid was 3.06, slightly lower than that of

https://dx.doi.org/10.1021/acssuschemeng.9b07479
ACS Sustainable Chem. Eng. XXXX, XXX, XXX−XXX

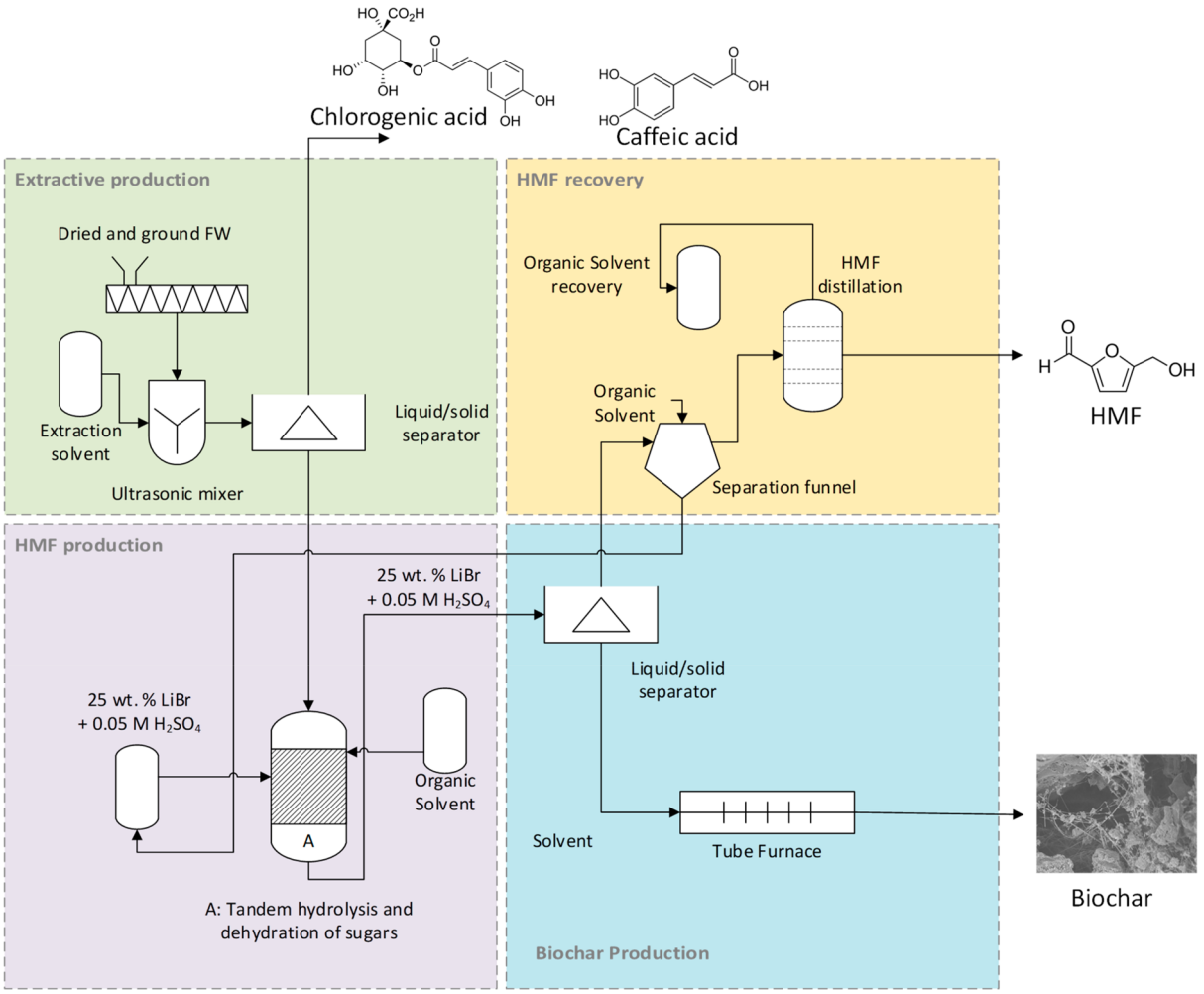

Figure 4. Blocks of proposed PPW valorization technology shown in colored boxes. In extraction, phenolic acids possessing antioxidant properties are extracted from the waste feedstock (green box). Carbohydrates are hydrolyzed and dehydrated (purple box) to yield a key platform chemical, HMF. HMF is separated from the organic solvent (yellow box). Finally, lignin is pyrolyzed into biochar (blue box).

Table 2. Total phenolic, DPPH, and ORAC contents of the PPE and PPW[a]

Tests	Values/g PPE	Values/g PPW
TPC, mg GAE	30.00 ± 0.54	6.90 ± 0.124
DPPH, m mol TE	0.0076 ± 0.0002	0.0017 ± 0.0005
ORAC, m mol TE	17.09 ± 0.33	3.93 ± 0.077

[a]Data shown are the means of at least three experiments ± standard (SD). Trolox equivalent (TE), 2,2-diphenyl-1-picrylhydrazyl (DPPH), and oxygen radical absorbance capacity (ORAC).

Innovator, *Russet*, and *Purple* potato varieties.[39] Further LC-MS is needed to ascertain the unknown peaks in the PPE chromatogram. Silva-Beltran et al.[37] reported DPPH and ORAC values for acidified ethanol extract as 0.38 and 4.00 m mol TE/g PPE, respectively, while the DPPH and ORAC values for their water extract were 0.1 and 5.31 m mol TE/g PPE respectively. Albishi et al.[39] reported an ORAC value ranging from 0.88−4.15 m mol TE/g PPW depending on potato variety. Our findings on ORAC of PPE were higher than reported values in both acidified ethanol and water PPE.

The PPE exhibits high antioxidant capacity as measured using the ORAC and DPPH radical scavenging assays (Table 2). These results highlight the potential of utilizing PPE for manufacturing dietary antioxidants with free radical scavenging capacities. This can provide a natural substitute to the widely used, petrochemically derived antioxidants, such as butylated hydroxyanisole (BHA) and butylated hydroxytoluene (BHT), which have been shown to be carcinogenic,[40,41] whereas natural antioxidants have been indicated to be noncarcinogenic and could be used in higher doses without adverse effects.[40] As the extractives are obtained from a food source, they can be used as is for dietary supplements, avoiding the use of flour fillers (increasing material cost) in current natural supplements.[42] Furthermore, ferulic acid can be isolated from the extractives and upgraded into biobased vanilla essence[43,44] as a potential product.

Conversion of Carbohydrates to HMF. For PPW saccharification, various loadings (1−8 wt %) of extracted PPW (PPW without extractives) were hydrolyzed in 25 wt % LiBr + 0.05 M H_2SO_4 at 140 °C. The addition of LiBr increases the solution Brønsted acidity by changing the activity coefficient of the solution.[45] In this work, we limited the amount of LiBr to 25 wt % (pH = 0 in 0.05 M H_2SO_4) to prevent pH lower than 0 and reduce the cost. High glucose yields were obtained (>80%); however, above 4 wt %, the glucose yield dropped below 80% (Figure S6). This could be due to mixing issues associated with the formation of a thick slurry at high PPW loading. A loading of 4 wt % was used for

https://dx.doi.org/10.1021/acssuschemeng.9b07479
ACS Sustainable Chem. Eng. XXXX, XXX, XXX−XXX

subsequent studies producing a glucose yield of ~90% within 1 h. After PPW saccharification, glucose dehydration to HMF was carried out in the same reactor. 2-Butanol was added to create a biphasic system in order to minimize HMF side reactions (Figure 5a). As shown in Figure 5a, starch is

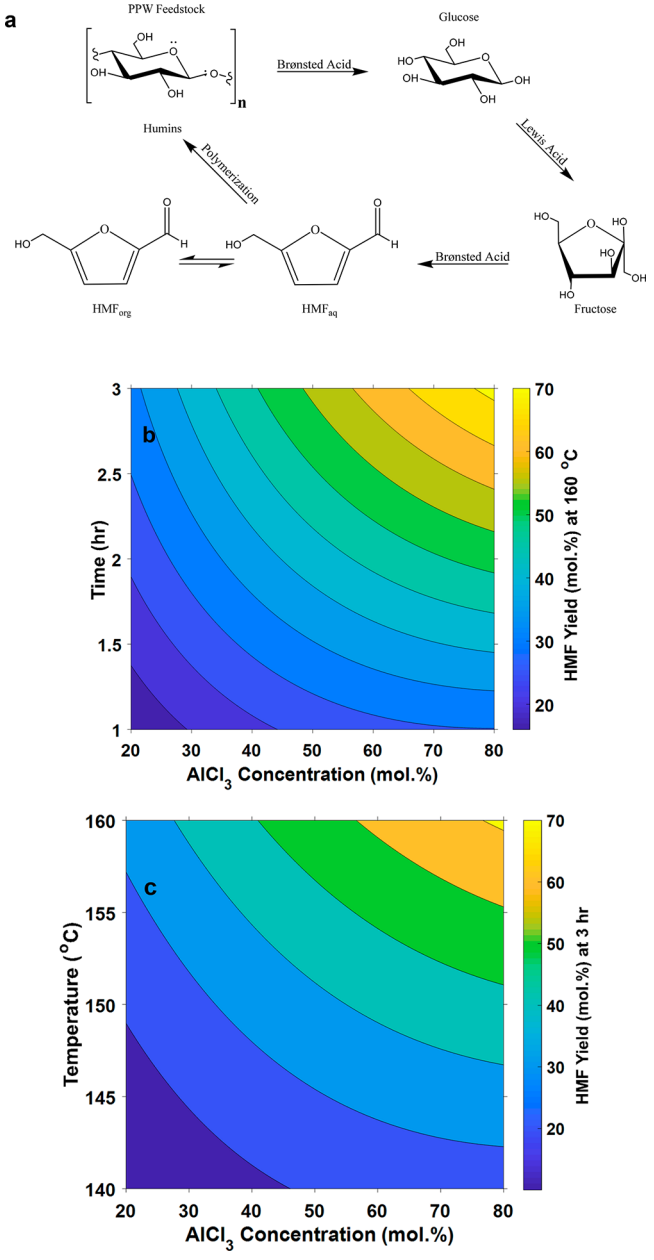

Figure 5. Dehydration of glucose to HMF. (a) Reaction pathways for acid-catalyzed saccharification and dehydration of PPW (containing glucan monomer units) to HMF in a biphasic system. (b) Effect of time-catalyst concentration on HMF yield at 160 °C. (c) Effect of temperature-catalyst concentration on HMF yield at 3 h. The color bar represents predicted HMF yield.

hydrolyzed to glucose using a Brønsted acid. Glucose is then isomerized to fructose in the presence of a Lewis acid ($AlCl_3$). Fructose is finally dehydrated using a Brønsted acid to produce HMF. Glucose dehydration to HMF has been carried out by varying temperature, reaction time,[46] and Lewis acid concentration.[47−54] The effects of these factors on glucose dehydration have typically been studied using a change-one-separate-factor at a time (COST) approach. This approach cannot account for synergistic or counteractive factor interactions on glucose dehydration. Thus, design of experiments was set up using a Box-Behnken design. The levels for each explored factor in the design are shown in Table S1.

The HMF yield was quantified for each of the 30 experiments (Table S2) and regressed with a polynomial model. The statistical significance of the model (see Supporting Information) was confirmed after comparing the *f*-statistic from the ANOVA and test table (Tables S4 and S5) evaluating the interpretability multiplier and the distribution of residuals (Figure S7). The pareto regression analysis plot (Figure S8) shows that all individual factors were significant, with time and temperature being the most significant ones influencing HMF yield (from coded magnitude of the factor coefficients). For the two-way interactions, $AlCl_3$ concentration−time and $AlCl_3$ concentration−temperature were identified as significant synergistic interactions on glucose dehydration into HMF. This highlights the utility of design of experiments for optimization, as COST cannot identify the contributions of factor-interactions, giving erroneous predictions of reaction optimum. Norton et al.[55] observed that the speciation of $AlCl_3$ in aqueous solution was affected by both temperature and time, supporting our finding on the synergistic two-factor interaction.

The response surface plots, which are the graphical results of interaction effects, are shown in Figure 5. Figure 5b,c shows the HMF yield surface plot as a function of time-catalyst concentration and temperature-catalyst concentration, respectively. Increased HMF yield is achieved with increasing temperature, time, and catalyst concentration. The contour plots depict a rising-ridge pattern with the highest yield being achieved at the maximum values of each factor. This indicates that further experimental testing (beyond explored factor levels in current design) could result in higher HMF yields. However, consideration needs to be given to the possibility that at elevated reaction temperatures (>160 °C), reactions to humins (Figure 5a) may be favored,[56] which can reduce HMF yield.

Microreactors may present an alternative to circumvent this challenge at very high temperatures due to short residence times.[57] The model predicted optimum temperature, time, and catalyst concentration are 160 °C, 3 h, and 80 mol % (Table S6), respectively. The optimum reaction conditions for HMF production were then applied to extracted PPW. A promisingly high HMF yield of 54 mol % (based on total glucan amount in PPW) was obtained directly from the extracted PPW (Figure S9); while some deviation from the predicted value is seen, the achieved yield is still sufficiently high. The HMF yield is higher than literature reported values for other food waste sources: 11 mol % from cooked rice and penne waste,[58] 19 mol % from kiwi and watermelon fruit waste,[58] and 30 mol % from bread waste.[59] For the recycle experiments, the aqueous phase, containing LiBr and Lewis acid $AlCl_3$, was recovered after separation of the organic phase containing HMF. This recovered solution was reused for starch hydrolysis and glucose dehydration in two more reaction cycles. The reused aqueous phase, containing 25 wt % LiBr + 0.05 M H_2SO_4 and Al species, yields a slightly lower amount HMF (50 mol %) in a third recycle. Our earlier work,[30] using ICP−MS analysis of the crude HMF, has shown partial loss of Li salt (reducing the effective acidity) into the organic phase, providing a possible reason for the lower HMF yield. Furanics, such as HMF, furfural, and furan itself, are ideal platforms[60] as they can be

https://dx.doi.org/10.1021/acssuschemeng.9b07479
ACS Sustainable Chem. Eng. XXXX, XXX, XXX−XXX

converted into a number of renewable, replacement and performance-advantaged bioproducts, such as aromatics, e.g., paraxylene,[61,62] toluene[63] and benzene[64] (BTX), dienes,[62] detergents,[65] lubricants[66−68] and fuels[69,70] which constitute part of the backbone of future bioenergy economy. These studies have also included process simulation with energy,[61] techno-economic,[66,69] and life cycle[69] assessment, demonstrating a clear environmental footprint impact. The economic viability is subject to crude oil price and can be competitive in some instances.

Thermal Characterization of Recovered PPW Residue. After producing HMF from the extracted PPW, the unreacted PPW residue (mainly lignin, ash, some unreacted carbohydrates, and humins) was recovered for pyrolysis into biochar. Thermogravimetric analysis (TGA) indicates a significant mass loss between 50−130 °C (Figure 6a), typically attributed to dewatering.[12] Evaporation of volatile compounds is usually observed between 130−200 °C. However, in our samples, no significant mass loss occurs within this temperature range, due to prior removal of volatile compounds, such as extractives, by solvent extraction. The increase in mass loss at ∼275 °C is attributed to the thermal decomposition of lignin. Decomposition of cellulose and lignin are associated with peaks at 375 and 420 °C, respectively. Similar TGA peaks were observed for thermal decomposition of raw PPW.[12]

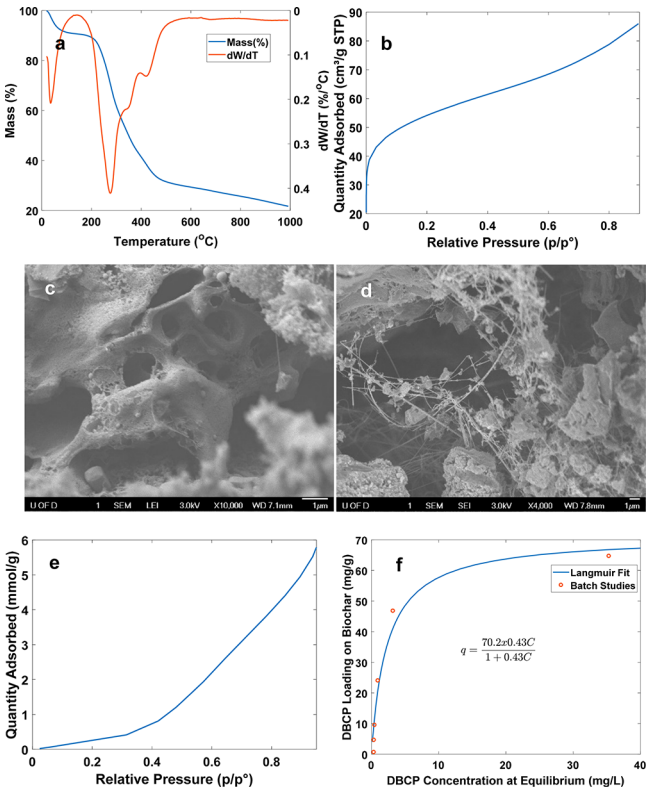

Figure 6. Characterization and analysis of synthesized biochar. (a) TGA (orange line) and DTG (blue line) thermograms of recovered PPW residue. (b) N_2 adsorption isotherm of PPW residue biochar. (c) Synthesized biochar showing porous structure. (d) Synthesized biochar showing web like nanofibre framework. (e) H_2O adsorption isotherm of PPW residue biochar. (f) Adsorption isotherm results for dibromochloropropane (DBCP) on PPW residue biochar.

Biochar Synthesis and Water Remediation. Biochar has various applications in manufacturing battery electrodes, carbon sequestration, filler for composites, catalysts, wastewater remediation, cofactor shuttling in anaerobic digestion, and soil amendment.[71] The biochar synthesis method (pyrolysis temperature, time, carrier gas, gas flow rate, and temperature ramping rate) determines the degree of graphitization, porosity, surface area, and surface phenolics, influencing its final application. The synthesis method applied here yields a highly porous and graphitic biochar. The biochar has a high Brunauer−Emmett−Teller (BET) surface area of 214 m^2/g, which can possibly be increased with further thermal or chemical activation. High nitrogen uptake at very low P/P^0 values (Figure 6b) is indicative of micropore filling. SEM imaging shows the presence of a hierarchical porous structure (Figure 6c) with interconnected carbon walls in the structure. Web-like nanofiber networks (Figure 6d) form around the bulk biochar. Such nanofibers have been reported[72,73] to form by deposition of volatiles (Table S7) released during pyrolysis of PPW residue on the biochar surface. They typically give rise to enhanced graphiticity. The biochar consists of macropores (>20 nm), mesopores (2−20 nm), and micropores (<2 nm), as shown in Figure S10. Minimal water adsorption (Figure 6e) indicates the material is hydrophobic. The increase in water uptake at higher relative pressures >0.3 is due to agglomeration of water molecules,[74] in the mesopores.[74] X-ray diffraction (XRD) (Figure S11) shows crystalline peaks attributed to graphite, silicon carbide, and potassium oxide, referenced from the international center for diffraction data (ICDD) database. The elemental composition, using energy dispersive X-ray spectroscopy (EDX) (Figure 3a), corroborates the XRD findings.

Owing to the hydrophobicity, graphiticity, and high surface area, we evaluated the potential of the synthesized biochar as an adsorbent of organic contaminants, and specifically, of a pesticide, 1, 2 dibromo-chloro-propane (DBCP) dissolved in deionized water. Batch isotherms (Figure 6f) were analyzed with a Langmuir isotherm shown in eq 1

$$q = \frac{q_m KC}{1 + KC} \tag{1}$$

where q = DBCP loading on biochar (mg/g) and C is the equilibrium concentration of DBCP (mg/L). The estimated values of q_m (maximum loading capacity) and K (equilibrium constant) are 70 mg/g and 0.43 L/mg, respectively. The value of q_m is comparable to previous DBCP-loading capacities of 102 mg/g[75] and 80−110 mg/g[76] using biochar from other feedstock. These results suggest that it is feasible to use PPW residue-based biochar for treatment of pesticide polluted water.

Techno-Economic Analysis of the Integrated FW Biorefinery. The Aspen Economic Analyzer V11 is used to perform economic assessment of the biorefinery. Simulation procedures, descriptions, and assumptions are outlined in the Supporting Information. According to the proposed process, 1 MT of dry PPW can be converted to 241 kg of extractives, 127 kg of HMF, and 47 kg of biochar (Figure 7a). These yields are significantly higher than those obtained by other technologies, such as the production of ethanol (348 kg of ethanol per MT PPW or 34.8 wt % yield)[13] or of lactic acid (250 kg of lactic acid per MT PPW or 25 wt % yield).[22]

Mass balances and utility consumption are given in Tables S8 and S9, respectively. The capital and operating cost is given in Table S10 and depicted in Figure S12, with breakdown of costs in Table S11. Around 20% of the capital cost is attributed to heat exchangers. Utility costs (primarily for heating reactors

https://dx.doi.org/10.1021/acssuschemeng.9b07479
ACS Sustainable Chem. Eng. XXXX, XXX, XXX−XXX

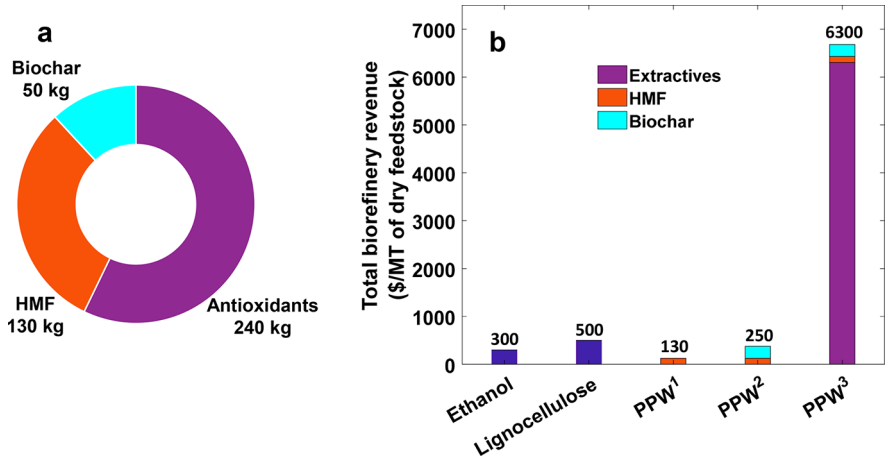

Figure 7. Results of techno-economic analysis. (a) Product distribution from PPW biorefinery. (b) Economic comparison of different integrated biorefineries. PPW[1] assumes HMF is the only product; PPW[2] assumes HMF and biochar are the only products; and PPW[3] assumes production of extractives, HMF, and biochar.

and biochar manufacture via pyrolysis) account for 38% of the operating cost. A lower pyrolysis temperature will result in less energy requirement and lower utility cost. Among processing steps, the hydrolysis and dehydration are the highest contributors to the operating and *annualized* capital costs. The capital costs can be reduced by better heat and energy integration within the plant.

We further compare the energy requirements for different biorefineries (Table S12 and Table S13). The energy requirements for biochemical based biorefineries, leading to ethanol[77,78] and biogas,[79,80] are much lower than biorefineries involving thermochemical transformations in the proposed FW-based and lignocellulose-based biorefineries[81] leading to more diverse bioproducts. The use of low fermentation temperatures (30−45 °C) and ambient pressure reduces utility costs. However, ethanol and biogas are high volume but low value products,[15] whereas molecules like furans and their derivatives, e.g., lubricants, are much more complex, lower volume/higher value products. Furthermore, biochemical transformations are inherently slow, requiring large reactors whereas thermochemical transformations of biomass can be very fast[57] and thus amenable to mobile processing. We use the ratio of revenue to energy input (REI) to compare these different refineries. This provides a fair comparison between the value of biorefinery products and energy required to make the products. Our FW biorefinery has a high REI ratio (Table S12) across the different biorefineries (almost three times that of a lignocellulose based biorefinery). This shows that high energy inputs (Table S12) required to manufacture high value products can be justified by the revenue made from sales. Efforts toward lower energy production of high value bioproducts should be a target for further biorefinery development.

The overall revenue of the process is $503 million per year, equivalent to $6280 per metric ton of dry PPW and results in a return on investment (ROI) of 2.0. Other economic profitability indices reveal a payback period of 0.5, making the technology attractive for investment. The best-case scenario uses an antioxidant market price of $25/kg. For a worst-case scenario, the minimum extractive price (MEP) for net profit >0 was calculated to be $14/kg. The payback period was calculated for various values of MEP (Figure S13). There is a transition from high to low price sensitivity (as observed in the change of the slope) around a MEP of $15/kg suggesting this as a good extractive selling price. At an MEP of $19/kg, the payback period is 1 year (annual net profit = total capital investment). Despite the high value of the antioxidant products, there is a high degree of uncertainty around its pricing. As shown in the sensitivity analysis (Figure S13), the profitability of the biorefinery is very sensitive to changes in the selling price of the extractive product. While the biobased HMF and biochar product market are more mature with stable product prices, the biobased antioxidant market is still nascent and requires further development to enable a robust and less volatile antioxidant pricing. Any viable biorefinery should have a low payback time (2−3 years) to minimize investment risk. At an extractive price of $15/kg, the payback period is 3.4 years indicating a conservative price for the extractives. Nevertheless, a robust market price analysis would be necessary to confirm these values. There is also a likelihood of price reduction driven by a glut effect from biobased antioxidants flooding the market. Therefore, two scenarios, excluding production of antioxidants, have also been evaluated. In the first scenario, HMF is taken as the only product and in the second scenario, HMF and biochar are the only products. With the biorefinery operating under these scenarios, the economics is still reasonable compared to other biorefinery processes. For the scenario including extractives production, the crude as obtained extractives yield is used in the TEA and economic calculations. Existing applications for antioxidants are in food, household products and as industrial additives. Yet, new applications as dietary supplements in the fitness and body building industry[82,83] could create a new antioxidant market segment to accommodate the flux of these naturally sourced antioxidants. Depending on the final application, further purification of the extractive product may be necessary, and this will increase the operating cost, reduce the overall revenue and increase the ROI. Therefore, a TEA on a pilot-scale of the technology would help refine these preliminary estimates. The biorefinery is assumed to be located close to the potato processing and distribution center, therefore we set the price of potato peels as zero. Including a "cost" for PPW, at a price of $100 per MT of PPW, indicates that the total cost of raw materials increases by 23%. While the net profit reduces by 12% and the payback period increases from 0.5 to 0.57 years. These results indicate that the predictions are robust and

https://dx.doi.org/10.1021/acssuschemeng.9b07479
ACS Sustainable Chem. Eng. XXXX, XXX, XXX−XXX

independent of whether PPW is free of charge or not. The operating cost increases by 12.4% by accounting for 1% mixing of the organic phase into the aqueous phase. In order to enhance the overall revenue of the biorefinery, increasing the HMF yield (Figure S14) would be a more attractive, rather than an equivalent increase in glucose yield.

This study shows the singular importance of utilizing FW feedstock toward economic feasibility and technology commercialization of a multiproduct biorefinery and represents a step toward commercialization of integrated biorefineries where FW and lignocellulose-plant material can be used symbiotically. Moreover, this technology provides a novel waste management approach, effectively diverting FW from landfills and reducing its environmental impact while creating commodity products that can penetrate existing and new markets. Attractiveness in investment can be increased by lowering sale prices of the commodity products below existing market values.

CONCLUSIONS

We have successfully shown that PPW can be repurposed as an alternative waste management strategy for manufacturing value-added products. With extractives, carbohydrates, and lignin components possessing different structures and reactivities, we effectively separate each component and process it into distinct renewable products. We report high antioxidant activity of PPE, providing a natural alternative to petrochemical-based antioxidants, with an end use as a dietary supplement or food preservative. Importantly, the optimized dehydration results in the highest reported yield of HMF (54 mol %) directly from PPW without sugar purification, reducing processing cost. The past decade has experienced tremendous expansion of the slate of bioproducts made from the platform HMF, one of which is recyclable biobased polymer made from furan dicarboxylic acid, an oxidation product of HMF. This knowledge can directly be harnessed for integrated biorefineries. The synthesized biochar is effective in removing pesticides from contaminated water. Biochar can store carbon in a stable form, preventing CO_2 from getting into the atmosphere, and a large quantity of it can be used for soil enrichment, which improves food security and crop production. Excitingly, the high-value products result in an overall revenue of $6300/MT of dry feedstock (Figure 7b), which is much higher than that of a cellulosic ethanol facility ($300/MT of dry feedstock)[84] or a lignocellulose based biorefinery ($500/MT of dry feedstock).[81] The favorable economics is driven by the high yield of PPE (20 wt % of PPW dry weight), coupled with the high value ($25 per kg of extract) of the antioxidant product. PPW manufacturing industries could generate revenues of ∼ $6300 per ton of PPW, compared to ∼$100 per ton of PPW when used for animal feed or incurring a landfill disposal cost of $400 per ton of PPW.[15] This provides an opportunity for successful translation of our technology to an economically profitable industry. This technology can be extended to other types of FW: banana peels, apple, and grape pomace,[85] as they contain similar components (lignin, extractives, and carbohydrates), and a larger range of bioproducts for the commodity market. What the analysis clearly indicates is that unlike lignocellulosic plant material, the unique compositions of some of the food waste, and specifically its extractives, offer unmatched opportunities for profitable integrated biorefineries while addressing a key environmental challenge by significantly reducing GHG emissions. Comparison of the revenue to energy input for biorefineries utilizing different feedstocks underscores the tremendous potential impact FW can play in the bioenergy economy.

ASSOCIATED CONTENT

Supporting Information

The Supporting Information is available free of charge at https://pubs.acs.org/doi/10.1021/acssuschemeng.9b07479.

Figures include potato production from 1960−2017, globally and in China + India, reactivity study of organic solvents with HMF, effect of solvent: water ratio on fraction of HMF extracted, H NMR signals for DBCP, chromatogram of standards and PPW extracts, effect of feedstock loading on glucose yield, residual plots for HMF yield, pareto chart of standardized effects on HMF yield, starch conversion to glucose and HMF yield from starch and PPW, pore size distribution of PPW residue biochar, XRD of PPW biochar, overview of cost and impact of raw materials, variation in payback period duration as a function of minimum extractive price, sensitivity Analysis (SA) for change in yield of glucose and HMF, flowsheet of HMF production from potato peels. Tables include peaks and phenolic compounds in the potato peel waste extracts solution, experimental factors levels for design of experiments, complete Box-Behnken design matrix for glucose dehydration, ANOVA table for Box-Behnken model, model summary, multiple response prediction, pyrolysis product distribution, material balances, utility consumption, summary of the capital and operating costs of the HMF process, breakdown of costs, REI ratios for different biorefineries, parameters used in computing revenue: energy index ratio, reaction specifications, raw material cost, product cost. Details on estimation of extractive price, evaluation of statistical significance of regression model techno-economics analysis (TEA) procedure, process description of the integrated FW biorefinery, assumptions for TEA are also provided (PDF)

AUTHOR INFORMATION

Corresponding Author

Dionisios G. Vlachos − *Catalysis Center for Energy Innovation and Department of Chemical and Biomolecular Engineering, University of Delaware, Newark, Delaware 19716, United States;* orcid.org/0000-0002-6795-8403; Email: vlachos@udel.edu

Authors

Elvis Ebikade − *Catalysis Center for Energy Innovation and Department of Chemical and Biomolecular Engineering, University of Delaware, Newark, Delaware 19716, United States*

Abhay Athaley − *Catalysis Center for Energy Innovation, University of Delaware, Newark, Delaware 19716, United States; Department of Chemical and Biochemical Engineering, Rutgers, The State University of New Jersey, Piscataway, New Jersey 08854, United States*

Benjamin Fisher − *Department of Chemical and Biomolecular Engineering, University of Delaware, Newark, Delaware 19716, United States*

https://dx.doi.org/10.1021/acssuschemeng.9b07479
ACS Sustainable Chem. Eng. XXXX, XXX, XXX−XXX

Kai Yang − *Department of Food Science and Technology, Zhejiang University of Technology, Hangzhou 310014, P. R. China; Department of Animal and Food Sciences, University of Delaware, Newark, Delaware 19716, United States*

Changqing Wu − *Department of Animal and Food Sciences, University of Delaware, Newark, Delaware 19716, United States;* orcid.org/0000-0003-4369-9045

Marianthi G. Ierapetritou − *Catalysis Center for Energy Innovation and Department of Chemical and Biomolecular Engineering, University of Delaware, Newark, Delaware 19716, United States;* orcid.org/0000-0002-1758-9777

Complete contact information is available at: https://pubs.acs.org/10.1021/acssuschemeng.9b07479

Notes

The authors declare no competing financial interest.

■ ACKNOWLEDGMENTS

This work was supported as part of the Catalysis Center for Energy Innovation, an Energy Frontier Research Center funded by the U.S. Department of Energy, Office of Science, and Office of Basic Energy Sciences under award number DE-SC0001004. E.E. also acknowledges support from the Allan and Myra Ferguson Fellowship. The authors also acknowledge the use of the Advanced Material Characterization Laboratory (AMCL) and the W.M. Keck Microscopy Facility at the University of Delaware. S. Sadula is thanked for providing supervision at the project initiation and assistance during PPW feedstock characterization. B. Saha is thanked for meaningful contributions and discussions during the project. J. Li and J. Hu is thanked for preliminary antioxidant analysis of our extracts. G. Poirer is thanked for training on several characterization techniques. N. R. Quiroz is thanked for assistance with NMR spectroscopy. J. Keeley is thanked for assistance with design of some figures in the manuscript.

■ REFERENCES

(1) Food and Agriculture Organization of the United Nations. Key facts on food loss and waste you should know! http://www.fao.org/save-food/resources/keyfindings/en/ (accessed Oct 28, 2019).

(2) The National Academies of Science Engineering and Medicine. *Science Breakthroughs to Advance Food and Agricultural Research by 2030*; The National Academies Press: Washington, DC, 2018. DOI: 10.17226/25059.

(3) U.S. Energy Information Administration. U.S. energy facts explained - consumption and production - U.S. Energy Information Administration (EIA) https://www.eia.gov/energyexplained/us-energy-facts/ (accessed Nov 16, 2019).

(4) Food and Agriculture Organization of the United Nations (FAO). Food Loss and Food Waste http://www.fao.org/food-loss-and-food-waste/en/ (accessed Jul 25, 2017).

(5) Gunders, D. *Wasted: How America Is Losing up to 40% of Its Food from Farm to Fork to Landfill*; **2012**. .

(6) United States Department of Agriculture; United States Environmental Protection Agency; United States Food and Drug Administration. *Formal Agreement Among the United States Environmental Protection Agency and the United States Food and Drug Administration and the United States Department of Agriculture Relative to Cooperation and Coordination on Food Loss and Waste*; **2018**.

(7) ReFED. *A Roadmap to Reduce U.S. Food Waste by 20%*; **2016**. DOI: 10.1017/CBO9781107415324.004.

(8) United States Environmental Protection Agency. *Industrial Food Processing Waste Analyses*; **2012**.

(9) Lin, C. S. K.; Pfaltzgraff, L. A.; Herrero-Davila, L.; Mubofu, E. B.; Abderrahim, S.; Clark, J. H.; Koutinas, A. A.; Kopsahelis, N.; Stamatelatou, K.; Dickson, F.; Thankappan, S.; Mohamed, Z.; Brocklesby, R.; Luque, R. Food Waste as a Valuable Resource for the Production of Chemicals, Materials and Fuels. Current Situation and Global Perspective. *Energy Environ. Sci.* **2013**, *6* (2), 426−464.

(10) Lim, X. Turning Organic Waste into Hydrogen. *ACS Cent. Sci.* **2019**, *5* (2), 203−205.

(11) Ogunbayo, A. O.; Olanipekun, O. O.; Ebikade, E. O. Evaluation of Bio-Methane Production from Abattoir Wastewater: Effect of Inoculum to Substrate Ratio (ISR) and Co-Digestion. *J. Solid Waste Technol. Manage.* **2017**, *43* (2), 83−90.

(12) Liang, S.; McDonald, A. G. Chemical and Thermal Characterization of Potato Peel Waste and Its Fermentation Residue as Potential Resources for Biofuel and Bioproducts Production. *J. Agric. Food Chem.* **2014**, *62* (33), 8421−8429.

(13) Arapoglou, D.; Varzakas, T.; Vlyssides, A.; Israilides, C. Ethanol Production from Potato Peel Waste (PPW). *Waste Manage.* **2010**, *30* (10), 1898−1902.

(14) Lin, C. S. K.; Koutinas, A. A.; Stamatelatou, K.; Mubofu, E. B.; Matharu, A. S.; Kopsahelis, N.; Pfaltzgraff, L. A.; Clark, J. H.; Papanikolaou, S.; Kwan, T. H.; Luque, R. Current and Future Trends in Food Waste Valorization for the Production of Chemicals, Materials and Fuels: A Global Perspective. *Biofuels, Bioprod. Biorefin.* **2014**, *8* (5), 686−715.

(15) Tuck, C. O.; Pérez, E.; Horváth, I. T.; Sheldon, R. A.; Poliakoff, M. Valorization of Biomass: Deriving More Value from Waste. *Science* **2012**, *337* (6095), 695−699.

(16) Buzby, J. C.; Farah-Wells, H.; Hyman, J. *Estimated Amount, Value, and Calories of Postharvest Food Losses at the Retail and Consumer Levels in the United States*; **2014**. DOI: 10.2139/ssrn.2501659.

(17) Bramsiepe, C.; Sievers, S.; Seifert, T.; Stefanidis, G. D.; Vlachos, D. G.; Schnitzer, H.; Muster, B.; Brunner, C.; Sanders, J. P. M.; Bruins, M. E.; Schembecker, G. Low-Cost Small Scale Processing Technologies for Production Applications in Various environments—Mass Produced Factories. *Chem. Eng. Process.* **2012**, *51*, 32−52.

(18) Hermann, B. G.; Blok, K.; Patel, M. K. Producing Bio-Based Bulk Chemicals Using Industrial Biotechnology Saves Energy and Combats Climate Change. *Environ. Sci. Technol.* **2007**, *41* (22), 7915−7921.

(19) Food and Agriculture Organization of the United Nations. FAOSTAT http://www.fao.org/faostat/en/#data/QC (accessed May 8, 2019).

(20) USDA ERS - Chart Detail https://www.ers.usda.gov/data-products/chart-gallery/gallery/chart-detail/?chartId=58340 (accessed Oct 23, 2019).

(21) United States Environmental Protection Agency. Greenhouse Gas Reporting Program (GHGRP) https://www.epa.gov/ghgreporting/ghgrp-waste (accessed Apr 4, 2019).

(22) Liang, S.; McDonald, A. G.; Coats, E. R. Lactic Acid Production from Potato Peel Waste by Anaerobic Sequencing Batch Fermentation Using Undefined Mixed Culture. *Waste Manage.* **2015**, *45*, 51−56.

(23) Ebikade, E.; Lym, J.; Wittreich, G.; Saha, B.; Vlachos, D. G. Kinetic Studies of Acid Hydrolysis of Food Waste-Derived Saccharides. *Ind. Eng. Chem. Res.* **2018**, *57* (51), 17365−17374.

(24) Pacific Northwest National Laboratory (PNNL) Top Value Added Chemicals from Biomass Volume I—Results of Screening for Potential Candidates from Sugars and Synthesis Gas Energy Efficiency and Renewable Energy. *NREL*; **2004**. DOI: 10.2172/15008859

(25) Lu, Y.; Wu, C. Reduction of Salmonella Enterica Contamination on Grape Tomatoes by Washing with Thyme Oil, Thymol, and Carvacrol as Compared with Chlorine Treatment. *J. Food Prot.* **2010**, *73* (12), 2270−2275.

(26) Wu, C.; Chen, F.; Wang, X.; Kim, H. J.; He, G. Q.; Haley-Zitlin, V.; Huang, G. Antioxidant Constituents in Feverfew (Tanacetum Parthenium) Extract and Their Chromatographic Quantification. *Food Chem.* **2006**, *96* (2), 220−227.

(27) Dong, X.; Dong, M.; Lu, Y.; Turley, A.; Jin, T.; Wu, C. Antimicrobial and Antioxidant Activities of Lignin from Residue of

Corn Stover to Ethanol Production. *Ind. Crops Prod.* **2011**, *34* (3), 1629−1634.
(28) Royal Society of Chemistry. GSK Solvent Selection Guide 2009. *Green Chem.* **2010**. DOI: 10.1039/c0gc00918k.
(29) Prat, D.; Wells, A.; Hayler, J.; Sneddon, H.; McElroy, R.; Peter, J. D.; Abou-Shehadad, S. CHEM21 Selection Guide of Classical- and Less Classical-Solvents. *Green Chem.* **2016**, *18*, 288−296.
(30) Sadula, S.; Athaley, A.; Zheng, W.; Ierapetritou, M.; Saha, B. Process Intensification for Cellulosic Biorefineries. *ChemSusChem* **2017**, *10* (12), 2566−2572.
(31) Sadula, S.; Oesterling, O.; Nardone, A.; Dinkelacker, B.; Saha, B. One-Pot Integrated Processing of Biopolymers to Furfurals in Molten Salt Hydrate: Understanding Synergy in Acidity. *Green Chem.* **2017**, *19* (16), 3888−3898.
(32) Van Den Bergh, J.; Babich, I. V.; O'Connor, P.; Moulijn, J. A. Production of Monosugars from Lignocellulosic Biomass in Molten Salt Hydrates: Process Design and Techno-Economic Analysis. *Ind. Eng. Chem. Res.* **2017**, *56* (45), 13423−13433.
(33) Sotillo, D. R.; Hadley, M.; Holm, E. T. Potato Peel Waste: Stability and Antioxidant Activity of a Freeze-Dried Extract. *J. Food Sci.* **1994**, *59* (5), 1031−1033.
(34) Singh, N.; Rajini, P.S. Free Radical Scavenging Activity of an Aqueous Extract of Potato Peel. *Food Chem.* **2004**, *85*, 611−616.
(35) Sotillo, D. R.; Hadley, M.; Wolf-Hall, C. Potato Peel Extract a Nonmutagenic Antioxidant with Potential Antimicrobial Activity. *J. Food Sci.* **1998**, *63* (5), 907−910.
(36) Samarin, A. M.; Poorazarang, H.; Hematyar, N.; Elhamirad, A. Phenolics in Potato Peels: Extraction and Utilization as Natural Antioxidants. *World Appl. Sci. J.* **2012**, *18* (2), 191−195.
(37) Silva-Beltrán, N. P.; Chaidez-Quiroz, C.; López-Cuevas, O.; Ruiz-Cruz, S.; López-Mata, M. A.; Del-Toro-Sánchez, C. L.; Marquez-Rios, E.; Ornelas-Paz, J. D. J. Phenolic Compounds of Potato Peel Extracts: Their Antioxidant Activity and Protection against Human Enteric Viruses. *J. Microbiol. Biotechnol.* **2017**, *27* (2), 234−241.
(38) Mohdaly, A. A. A.; Hassanien, M. F. R.; Mahmoud, A.; Sarhan, M. A.; Smetanska, I. Phenolics Extracted from Potato, Sugar Beet, and Sesame Processing by-Products. *Int. J. Food Prop.* **2013**, *16* (5), 1148−1168.
(39) Albishi, T.; John, J. A.; Al-Khalifa, A. S.; Shahidi, F. Phenolic Content and Antioxidant Activities of Selected Potato Varieties and Their Processing by-Products. *J. Funct. Foods* **2013**, *5* (2), 590−600.
(40) Kahl, R.; Kappus, H. Toxikologie Der Synthetischen Antioxidantien BHA Und BHT Im Vergleich Mit Dem Natürlichen Antioxidans Vitamin E. *Z. Lebensm.-Unters. Forsch.* **1993**, *196* (4), 329−338.
(41) Ito, N.; Fukushima, S.; Tsuda, H. Carcinogenicity and Modification of the Carcinogenic Response by BHA, BHT, and Other Antioxidants. *CRC Crit. Rev. Toxicol.* **1985**, *15* (2), 109−150.
(42) Super Antioxidants Veg Capsules | NOW Foods https://www.nowfoods.com/supplements/super-antioxidants-veg-capsules (accessed Jan 4, 2020).
(43) BASF. Making a difference in the natural F&F ingredients market https://www.basf.com/global/en/products/segments/nutrition_and_care/nutrition_and_health/aroma-ingredients/our_product_range/flavor-and-fragrance-ingredients.html (accessed Jan 28, 2020).
(44) Solvay. Solvay offers the vanillin the food industry wants today | Solvay https://www.solvay.com/en/article/natural-vanillin-ensures-resource-efficiency (accessed Jan 28, 2020).
(45) Rodriguez Quiroz, N.; Padmanathan, A. M. D.; Mushrif, S. H.; Vlachos, D. G. Understanding Acidity of Molten Salt Hydrate Media for Cellulose Hydrolysis by Combining Kinetic Studies, Electrolyte Solution Modeling, Molecular Dynamics Simulations, and ^{13}C NMR Experiments. *ACS Catal.* **2019**, *9* (11), 10551−10561.
(46) Pagán-Torres, Y. J.; Wang, T.; Gallo, J. M. R.; Shanks, B. H.; Dumesic, J. A. Production of 5-Hydroxymethylfurfural from Glucose Using a Combination of Lewis and Brønsted Acid Catalysts in Water in a Biphasic Reactor with an Alkylphenol Solvent. *ACS Catal.* **2012**, *2* (6), 930−934.
(47) Cai, C. M.; Nagane, N.; Kumar, R.; Wyman, C. E. Coupling Metal Halides with a Co-Solvent to Produce Furfural and 5-HMF at High Yields Directly from Lignocellulosic Biomass as an Integrated Biofuels Strategy. *Green Chem.* **2014**, *16*, 3819−3829.
(48) Insyani, R.; Verma, D.; Kim, S. M.; Kim, J. Direct One-Pot Conversion of Monosaccharides into High-Yield 2,5-Dimethylfuran over a Multifunctional Pd/Zr-Based Metal-organic Framework Sulfonated Graphene Oxide Catalyst. *Green Chem.* **2017**, *19*, 2482−2490.
(49) Wang, C.; Zhang, L.; Zhou, T.; Chen, J.; Xu, F. Synergy of Lewis and Brønsted Acids on Catalytic Hydrothermal Decomposition of Carbohydrates and Corncob Acid Hydrolysis Residues to 5-Hydroxymethylfurfural. *Sci. Rep.* **2017**, *7* (40908), 1−9.
(50) Chheda, J. N.; Roman-Leshkov, Y.; Dumesic, J. a. Production of 5-Hydroxymethylfurfural and Furfural by Dehydration of Biomass-Derived Mono- and Poly-Saccharides. *Green Chem.* **2007**, *9* (4), 342−350.
(51) Dallas Swift, T.; Nguyen, H.; Anderko, A.; Nikolakis, V.; Vlachos, D. G. Tandem Lewis/Brønsted Homogeneous Acid Catalysis: Conversion of Glucose to 5-Hydoxymethylfurfural in an Aqueous Chromium Iii Chloride and Hydrochloric Acid Solution. *Green Chem.* **2015**, *17* (10), 4725−4735.
(52) Enslow, K. R.; Bell, A. T. $SnCl_4$ -Catalyzed Isomerization/dehydration of Xylose and Glucose to Furanics in Water. *Catal. Sci. Technol.* **2015**, *5* (5), 2839−2847.
(53) Choudhary, V.; Mushrif, S. H.; Ho, C.; Anderko, A.; Nikolakis, V.; Marinkovic, N. S.; Frenkel, A. I.; Sandler, S. I.; Vlachos, D. G. Insights into the Interplay of Lewis and Brønsted Acid Catalysts in Glucose and Fructose Conversion to 5-(Hydroxymethyl)furfural and Levulinic Acid in Aqueous Media. *J. Am. Chem. Soc.* **2013**, *135* (10), 3997−4006.
(54) Murzin, D. Y.; Murzina, E. V.; Aho, A.; Kazakova, M. A.; Selyutin, A. G.; Kubicka, D.; Kuznetsov, V. L.; Simakova, I. L. Aldose to Ketose Interconversion: Galactose and Arabinose Isomerization over Heterogeneous Catalysts. *Catal. Sci. Technol.* **2017**, *7*, 5321−5331.
(55) Norton, A. M.; Nguyen, H.; Xiao, N. L.; Vlachos, D. G. Direct Speciation Methods to Quantify Catalytically Active Species of AlCl3 in Glucose Isomerization. *RSC Adv.* **2018**, *8* (31), 17101−17109.
(56) Cheng, Z.; Everhart, J. L.; Tsilomelekis, G.; Nikolakis, V.; Saha, B.; Vlachos, D. G. Structural Analysis of Humins Formed in the Brønsted Acid Catalyzed Dehydration of Fructose. *Green Chem.* **2018**, *20* (5), 997−1006.
(57) Desir, P.; Saha, B.; Vlachos, D. G. Ultrafast Flow Chemistry for the Acid-Catalyzed Conversion of Fructose. *Energy Environ. Sci.* **2019**, *12* (8), 2463−2475.
(58) Yu, I. K. M.; Tsang, D. C. W.; Yip, A. C. K.; Chen, S. S.; Ok, Y. S.; Poon, C. S. Valorization of Starchy, Cellulosic, and Sugary Food Waste into Hydroxymethylfurfural by One-Pot Catalysis. *Chemosphere* **2017**, *184*, 1099−1107.
(59) Yu, I. K. M.; Tsang, D. C. W.; Yip, A. C. K.; Chen, S. S.; Wang, L.; Ok, Y. S.; Poon, C. S. Catalytic Valorization of Starch-Rich Food Waste into Hydroxymethylfurfural (HMF): Controlling Relative Kinetics for High Productivity. *Bioresour. Technol.* **2017**, *237*, 222−230.
(60) Wang, T.; Nolte, M. W.; Shanks, B. H. Catalytic Dehydration of C_6 Carbohydrates for the Production of Hydroxymethylfurfural (HMF) as a Versatile Platform Chemical. *Green Chem.* **2014**, *16* (2), 548−572.
(61) Athaley, A.; Annam, P.; Saha, B.; Ierapetritou, M. Techno-Economic and Life Cycle Analysis of Different Types of Hydrolysis Process for the Production of P-Xylene. *Comput. Chem. Eng.* **2019**, *121*, 685−695.
(62) Williams, C. L.; Chang, C. C.; Do, P.; Nikbin, N.; Caratzoulas, S.; Vlachos, D. G.; Lobo, R. F.; Fan, W.; Dauenhauer, P. J. Cycloaddition of Biomass-Derived Furans for Catalytic Production of Renewable P -Xylene. *ACS Catal.* **2012**, *2* (6), 935−939.
(63) Green, S. K.; Patet, R. E.; Nikbin, N.; Williams, C. L.; Chang, C.-C.; Yu, J.; Gorte, R. J.; Caratzoulas, S.; Fan, W.; Vlachos, D. G.;

https://dx.doi.org/10.1021/acssuschemeng.9b07479
ACS Sustainable Chem. Eng. XXXX, XXX, XXX−XXX

Dauenhauer, P. J. Diels-Alder Cycloaddition of 2-Methylfuran and Ethylene for Renewable Toluene. *Appl. Catal., B* **2016**, *180*, 487−496.
(64) Koehle, M.; Saraçi, E.; Dauenhauer, P.; Lobo, R. F. Production of P-Methylstyrene and P-Divinylbenzene from Furanic Compounds. *ChemSusChem* **2017**, *10* (1), 91−98.
(65) Park, D. S.; Joseph, K. E.; Koehle, M.; Krumm, C.; Ren, L.; Damen, J. N.; Shete, M. H.; Lee, H. S.; Zuo, X.; Lee, B.; Fan, W.; Vlachos, D. G.; Lobo, R. F.; Tsapatsis, M.; Dauenhauer, P. J. Tunable Oleo-Furan Surfactants by Acylation of Renewable Furans. *ACS Cent. Sci.* **2016**, *2* (11), 820−824.
(66) Liu, S.; Josephson, T. R.; Athaley, A.; Chen, Q. P.; Norton, A.; Ierapetritou, M.; Siepmann, J. I.; Saha, B.; Vlachos, D. G. Renewable Lubricants with Tailored Molecular Architecture. *Sci. Adv.* **2019**, *5* (2), 1−8.
(67) Liu, S.; Dutta, S.; Zheng, W.; Gould, N. S.; Cheng, Z.; Xu, B.; Saha, B.; Vlachos, D. G. Catalytic Hydrodeoxygenation of High Carbon Furylmethanes to Renewable Jet-Fuel Ranged Alkanes over a Rhenium-Modified Iridium Catalyst. *ChemSusChem* **2017**, *10* (16), 3225−3234.
(68) Norton, A. M.; Liu, S.; Saha, B.; Vlachos, D. G. Branched Bio-Lubricant Base Oil Production via Aldol Condensation. *ChemSusChem* **2019**, *12* (21), 4780−4785.
(69) Athaley, A.; Saha, B.; Ierapetritou, M. Biomass-based Chemical Production Using Techno-economic and Life Cycle Analysis. *AIChE J.* **2019**, *65* (9), 1−15.
(70) Gumidyala, A.; Wang, B.; Crossley, S. Direct Carbon-Carbon Coupling of Furanics with Acetic Acid over Brønsted Zeolites. *Sci. Adv.* **2016**, *2* (9), 1−8.
(71) Weber, K.; Quicker, P. Properties of Biochar. *Fuel* **2018**, *217*, 240−261.
(72) Wang, F. J.; Zhang, S.; Chen, Z. D.; Liu, C.; Wang, Y. G. Tar Reforming Using Char as Catalyst during Pyrolysis and Gasification of Shengli Brown Coal. *J. Anal. Appl. Pyrolysis* **2014**, *105*, 269−275.
(73) Hosokai, S.; Norinaga, K.; Kimura, T.; Nakano, M.; Li, C. Z.; Hayashi, J. I. Reforming of Volatiles from the Biomass Pyrolysis over Charcoal in a Sequence of Coke Deposition and Steam Gasification of Coke. *Energy Fuels* **2011**, *25* (11), 5387−5393.
(74) Liu, L.; Tan, S. J.; Horikawa, T.; Do, D.D.; Nicholson, D.; Liu, J. Water Adsorption on Carbon - A Review. *Adv. Colloid Interface Sci.* **2017**, *250*, 64−78.
(75) Klasson, K. T.; Ledbetter, C. A.; Uchimiya, M.; Lima, I. M. Activated Biochar Removes 100% Dibromochloropropane from Field Well Water. *Environ. Chem. Lett.* **2013**, *11* (3), 271−275.
(76) Thomas Klasson, K.; Ledbetter, C. A.; Wartelle, L. H.; Lingle, S. E. Feasibility of Dibromochloropropane (DBCP) and Trichloroethylene (TCE) Adsorption onto Activated Carbons Made from Nut Shells of Different Almond Varieties. *Ind. Crops Prod.* **2010**, *31* (2), 261−265.
(77) Sheldon, R. A. The Road to Biorenewables: Carbohydrates to Commodity Chemicals. *ACS Sustainable Chem. Eng.* **2018**, *6* (4), 4464−4480.
(78) Lorenz, D.; Morris, D. *How Much Energy Does It Take to Make a Gallon of Ethanol?*; Minneapolis, 1992.
(79) Cherubini, F.; Bird, N. D.; Cowie, A.; Jungmeier, G.; Schlamadinger, B.; Woess-Gallasch, S. Energy-and Greenhouse Gas-Based LCA of Biofuel and Bioenergy Systems: Key Issues. *Ranges and Recommendations.* **2009**, *53*, 434−447.
(80) Ministry of Agriculture and Food and Rural Affairs. Energy Yields from a Farm-Based Anaerobic Digestion System http://www.omafra.gov.on.ca/english/engineer/facts/enyields.htm#6 (accessed Sep 11, 2019).
(81) Alonso, D. M.; Hakim, S. H.; Zhou, S.; Won, W.; Hosseinaei, O.; Tao, J.; Garcia-Negron, V.; Motagamwala, A. H.; Mellmer, M. A.; Huang, K.; Houtman, C. J.; Labbé, N.; Harper, D. P.; Maravelias, C. T.; Runge, T.; Dumesic, J. A. Increasing the Revenue from Lignocellulosic Biomass: Maximizing Feedstock Utilization. *Sci. Adv.* **2017**, *3* (5), 1−7.
(82) Antioxidants | bodybuilding.com https://www.bodybuilding.com/store/antiox.html (accessed Nov 16, 2019).
(83) Bentley, D.; Ackerman, J.; Clifford, T.; Slattery, K. Acute and Chronic Effects of Antioxidant Supplementation on Exercise Performance. In *Antioxidants in Sport Nutrition*; CRC Press, 2014; pp 141−154. DOI: 10.1201/b17442-10.
(84) Lane, J. Unorthodox antioxidant focus drives Stover Ventures towards cellulosic dream: Biofuels Digest http://www.biofuelsdigest.com/bdigest/2018/08/22/unorthodox-antioxidant-focus-drives-stover-ventures-towards-cellulosic-dream/ (accessed Sep 27, 2018).
(85) Gowman, A. C.; Picard, M. C.; Rodriguez-Uribe, A.; Misra, M.; Khalil, H.; Thimmanagari, M.; Mohanty, A. K. Physicochemical Analysis of Apple and Grape Pomaces. *BioResources* **2019**, *14* (2), 3210−3230.

https://dx.doi.org/10.1021/acssuschemeng.9b07479
ACS Sustainable Chem. Eng. XXXX, XXX, XXX−XXX